SUPPORTING INFORMATION

Highly scalable production of uniformly-coated superparamagnetic nanoparticles for triggered drug release from alginate hydrogels

Alexandra Teleki[1], *Florian L. Haufe*[1], *Ann M. Hirt*[3], *Sotiris E. Pratsinis*[1], *Georgios A. Sotiriou*[1,2]*

[1]Particle Technology Laboratory, Institute of Process Engineering, Department of Mechanical and Process Engineering, ETH Zurich, Sonneggstrasse 3, CH-8092 Zurich, Switzerland.
[2]Drug Formulation & Delivery, Institute of Pharmaceutical Sciences, Department of Chemistry and Applied Biosciences, ETH Zurich, Vladimir-Prelog-Weg 3, CH-8093 Zurich, Switzerland.
[3]Institute of Geophysics, Department of Earth Sciences, ETH Zurich, Sonneggstrasse 5, CH-8092 Zurich, Switzerland.

15 February 2016

Submitted to:

RSC Advances

*Corresponding author: georgios.sotiriou@pharma.ethz.ch

Alginate purification

Below a schematic process diagram of the alginate purification process is shown.

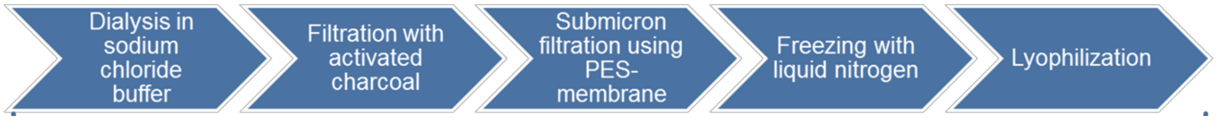

In Figure S1, two pictures of alginates before (a) and after (b) purification are shown. While off-the-shelf alginates are fine powders with a pale brown color, purified alginates are bright white foams. Both samples depicted have a mass of approximately 130 mg. As seen in picture (b), the purified alginate has a notably lower density (~6.7 mg/cm^3) due to the water sublimation during lyophilization. When prepared as aqueous solutions, notably different colors can be also observed. Unpurified alginate solutions are yellow and less transparent compared to the colorless purified solutions. About 60 % to 80 % of the initially dissolved, unpurified alginate can be retrieved in purified state at the end of the process.

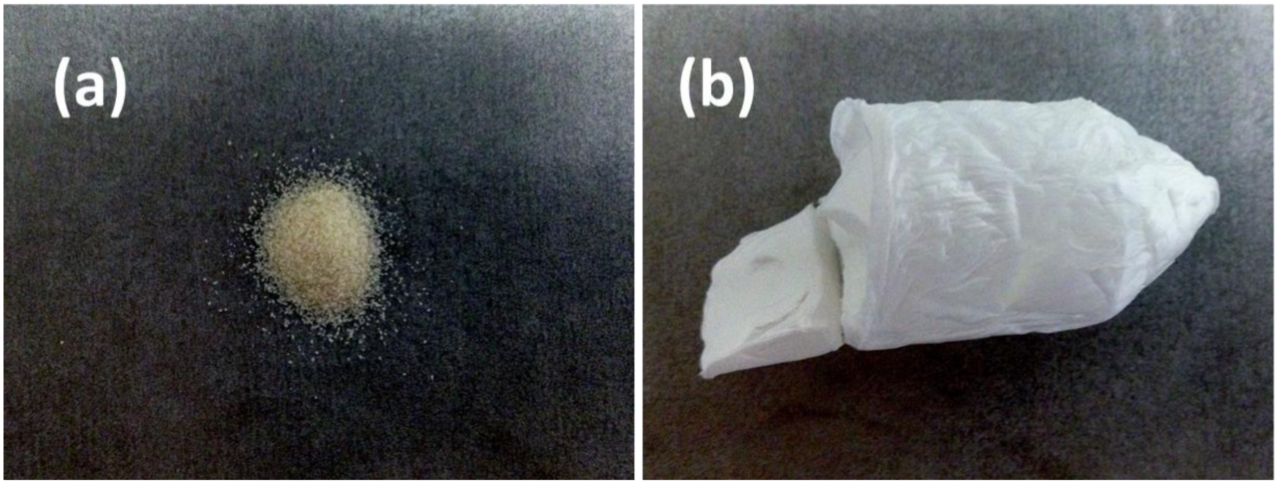

Figure S1. Pictures of unpurified alginate (a) and of alginate after purification (b). The two pictures have the same spatial scale and both show approximately 130 mg of alginate. A notable color change from yellowish to bright white can be observed. Due to the freeze-drying, the density of the sample after purification (b) is very low.

Sink conditions

The dextran-FITC release from the alginate beads was investigated in 3 different vessel volumes, at 1.5, 3 and 6 mL in order to ensure that the release occurs in sink conditions. Figure S2 shows the release after 4 h as a function of the vessel volume. The release at 3 and 6 mL volume reaches similar values at all three temperatures, indicating that 3 mL is the minimum vessel volume to ensure sink conditions.

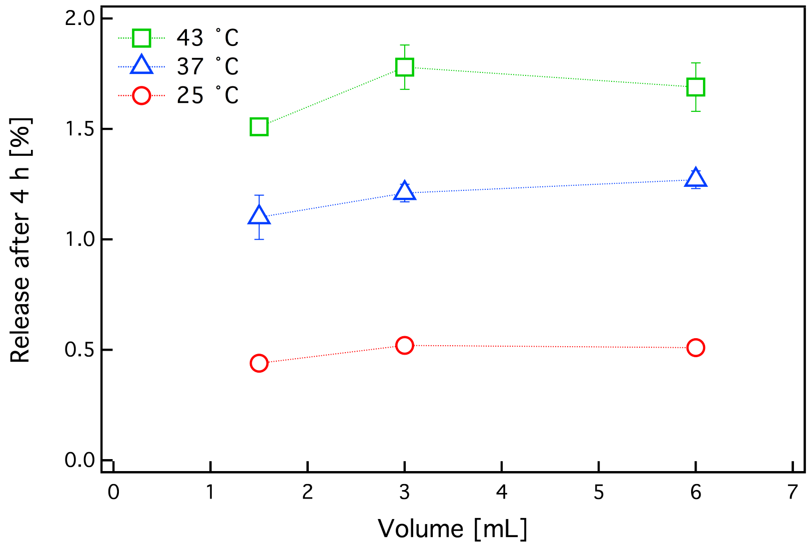

Figure S2. DEAE-dextran-FITC release from alginate beads after 4 h as a function of the vessel volume

Dextran calibration curves

The fluorescence light emission of samples containing known amounts of FITC-labeled dextran was measured with a spectrophotometer to correlate emission intensity with dextran concentration. Two completely independent sets of standard samples were prepared. One standard set (“reference”) was used to gather data based on which a least square linear regression could be obtained. The quality of the fit was then verified using the other standard set (“verification”). Figure S3 shows the reference data, verification data, and the linear fit calculated based on the reference data for methods M4 and M5. Each method corresponds to two different concentration ranges. For low dextran concentrations that are particularly prone to measurement errors, higher excitation voltages can be applied (method M4 and M5 had voltages 400 and 435 V, respectively) to obtain a more steeply inclined linear fit. Consequently, errors of the same magnitude in the intensity measurements will result in smaller errors in the concentration readings. As indicated by the very strong correlations between the linear fit and the verification sets, spectrophotometry is capable of highly accurate concentration measurements.

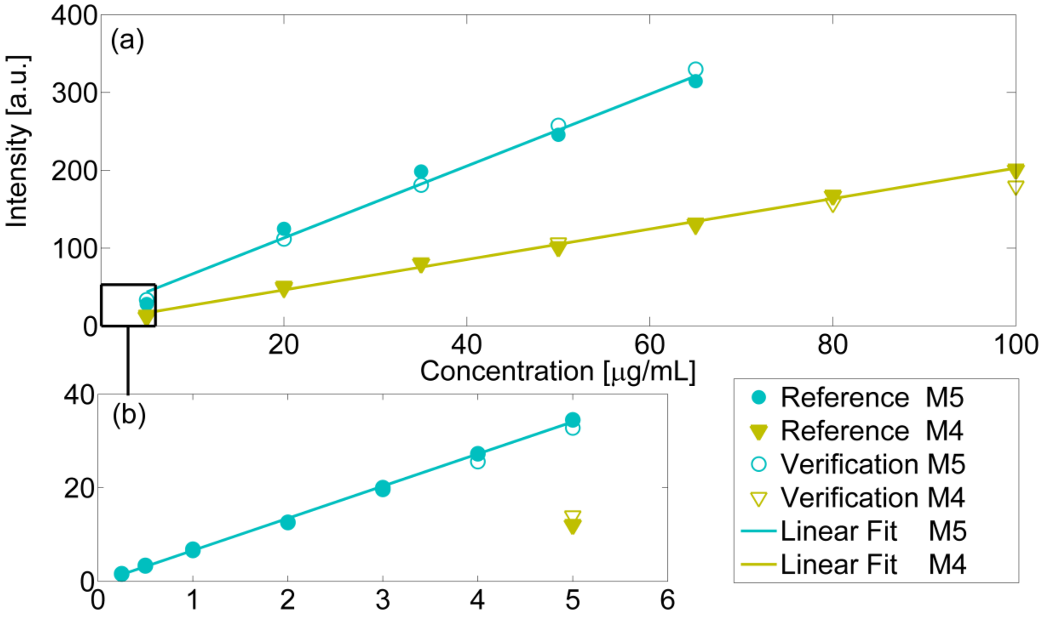

Figure S3. Spectrophotometer calibration for FITC-dextran detection. Filled symbols are reference measurements based on which linear fits (solid lines) were obtained. Verification measurements (open symbols, sometimes obscured by filled symbols) were performed to assess the degree of correlation between intensity and dextran concentration. For both methods, R^2 values of the linear fits are > 0.98.

X-ray diffraction analysis and reproducibility

Figure S4 shows a comparison of XRD patterns for the flame-made SiO_2-coated Fe_2O_3 nanoparticles used in this study (black and red lines) with particles from the literature (blue line, from Teleki et al.). As expected, the very close agreement between the different patterns in terms of peak position and height indicates maghemite as the dominant crystal phase. Small amounts of hematite may have formed due to the high temperature regime in the enclosed FSP reactor used. The presence of magnetite in products made with this FSP set-up is rather unlikely, because the oxygen-rich environment in the flame reactor favors the formation of maghemite. XRD analysis of two independent samples made at identical conditions (red and blue lines) yields an almost identical crystal size of 19 and 18 nm, respectively. These values are slightly larger than the 15 nm measured by Teleki et al.

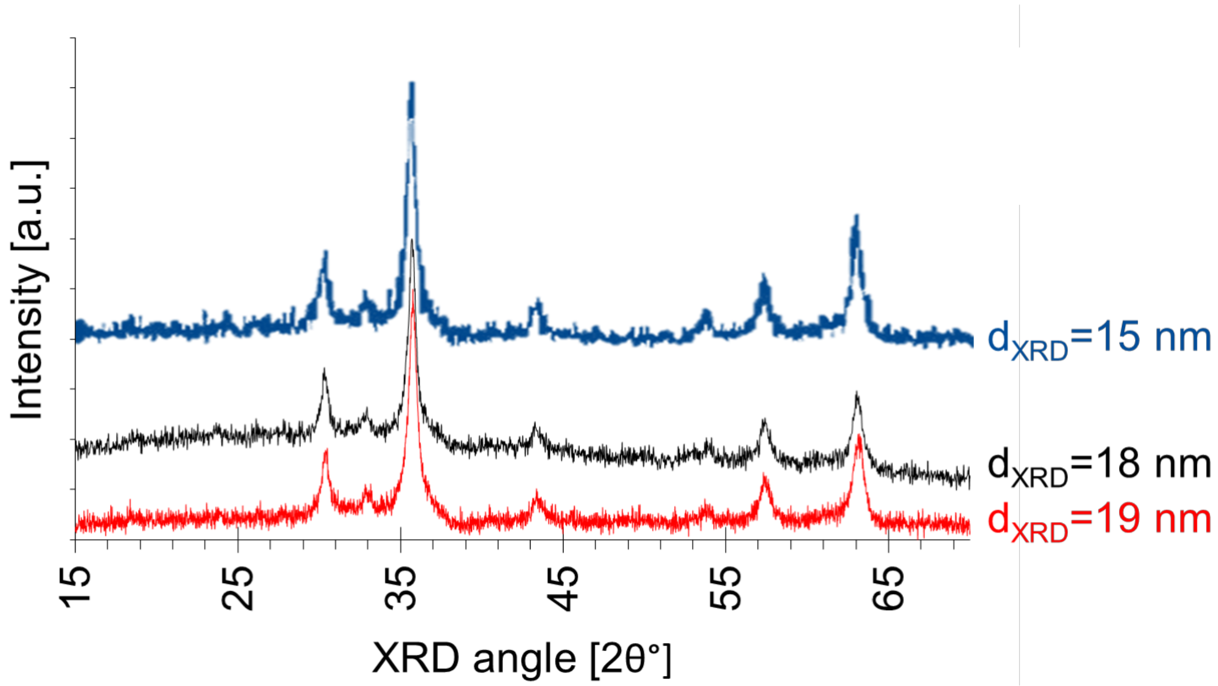

Figure S4. XRD-patterns and primary crystal sizes of SiO_2-coated Fe_2O_3 nanoparticles from Teleki et al. (blue line), and two independent samples from this work (black and red lines). Peak positions and relative heights agree very well, indicating maghemite as predominantly present crystal phase.

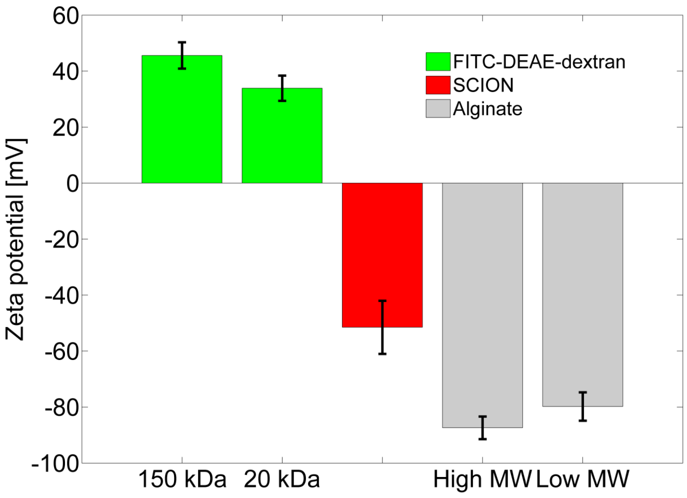

Figure S5. Zeta-potentials of 150 kDa and 20 kDa FITC-DEAE-dextrans, SiO_2-coated Fe_2O_3 nanoparticles and high and low MW alginate. A strong mutual attraction of alginate and FITC-DEAE-dextran can be expected due to the potential gradient of more than 100 mV.

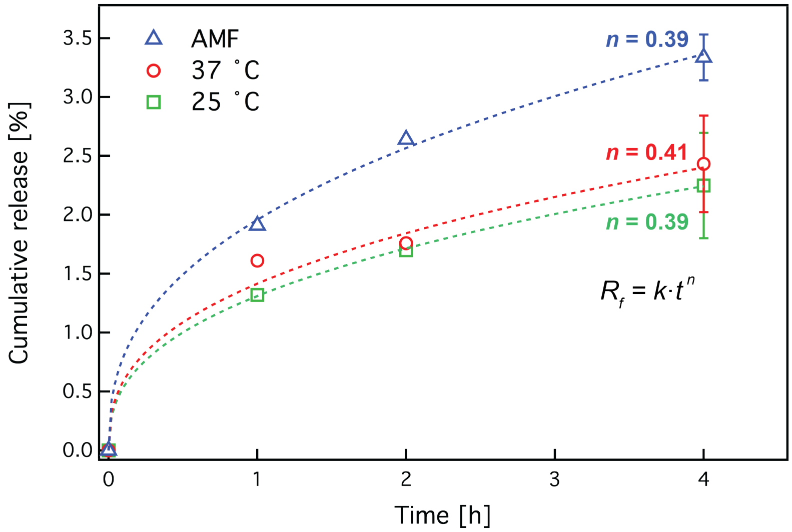

Figure S6. Cumulative release of dextran-FITC from the superparamagnetic alginate beads as a function of time for alginate suspensions incubated at 25 (green squares), 37 ˚C (red circles) and in the presence of an alternating magnetic field (AMF, blue triangles). Power law equation fits of each profile are shown with broken lines. Error bars correspond to standard deviation of three measurements. The cumulative release in the presence of AMF is enhanced.

References

A. Teleki, M. Suter, P. R. Kidambi, O. Ergeneman, F. Krumeich, B. J. Nelson, S. E. Pratsinis, *Chem. Mater.,* 2009, **21**(10), 2094-2100.